# Allan Deviation Plot as a Tool for Quartz-Enhanced Photoacoustic Sensors Noise Analysis

Marilena Giglio, Pietro Patimisco, Angelo Sampaolo, Gaetano Scamarcio, Frank K. Tittel, and Vincenzo Spagnolo

***Abstract*—We report here on the use of the Allan deviation plot to analyze the long-term stability of a quartz-enhanced photoacoustic (QEPAS) gas sensor. The Allan plot provides information about the optimum averaging time for the QEPAS signal and allows the prediction of its ultimate detection limit. The Allan deviation can also be used to determine the main sources of noise coming from the individual components of the sensor. Quartz tuning fork thermal noise dominates for integration times up to 275 s, whereas at longer averaging times, the main contribution to the sensor noise originates from laser power instabilities.**

***Index Terms*—Gas detectors, laser noise, noise measurement, optical sensors, thermal noise.**

## I. Introduction

ENVIRONMENTAL monitoring, industrial process control analysis, breath diagnostics, and security are just a few of the many fields of gas sensing applications requiring ever increasing improvements in sensitivity and selectivity [1]. Quartz-enhanced photoacoustic spectroscopy (QEPAS) is one of the most robust and sensitive trace-gas optical detection techniques. This method is based on photoacoustic effect, i.e., heat conversion of light absorbed by a gas target via molecular collision-induced nonradiative relaxation of excited states [2]. This heating causes the gas to expand and, if the light is modulated, the periodic expansion produces pressure waves, i.e., sound that can be detected. QEPAS is based on the use of a quartz tuning fork (QTF) resonator as an optoacoustic transducer and the frequency of light modulation has to match the QTF resonance frequency or one of its subharmonics. QEPAS is capable of extremely high detection sensitivities with a compact and relatively low-cost absorption detection module [3], [4]. Sensitivity represents a crucial figure of merit in any sensor system, and for QEPAS corresponds to the gas concentration providing a signal equivalent to the noise [signal-to-noise ratio $(\mathrm{SNR} = 1)$]. Thus, the sensitivity of a QEPAS sensor can be improved by further averaging its signal. From a theoretical point of view, the signal from a perfectly stable system could be infinitely averaged, thus leading to extremely sensitive measurements. However, an optical sensor operating in the field is a limited stable system. There exists an optimum integration time at which the detection limit reaches a minimum value. At longer averaging time, drift effects emerge and the sensor performance deteriorates. The optimum integration time is both application—and installation—specific for a given sensor instrument. The Allan variance analysis allows the determination of how long optical sensor signals can be averaged to increase the detection sensitivity, and before noise sources like laser instability, temperature, and mechanical drifts, as well as when moving fringes begin to dominate. This technique was initially developed by Allan in 1966 to study the frequency stability of precision oscillators [5]. In 1993, Werle applied the Allan variance to signal averaging in tunable laser absorption spectroscopy (TDLAS) instrumentation [6]. In this paper, we apply this approach to a QEPAS gas sensor to determine the main source of instabilities and the resulting optimum integration time.

Manuscript received June 8, 2015; accepted August 25, 2015. Date of publication October 27, 2015; date of current version April 1, 2016. The work of M. Giglio, P. Patimisco, A. Sampaolo, G. Scamarcio, and V. Spagnolo was supported by three Italian research projects: PON02 00675, PON02 00576, and PON03—SISTEMA.

M. Giglio, P. Patimisco, A. Sampaolo, G. Scamarcio, and V. Spagnolo are with the Dipartimento Interateneo di Fisica, Università e Politecnico di Bari, CNR-IFN UOS BARI, Bari I-70020, Italy (e-mail: vincenzo.spagnolo@uniba.it).

F. K. Tittel is with the Department of Electrical and Computer Engineering, Rice University, Houston, TX 77005 USA (e-mail: fkt@rice.edu).

Digital Object Identifier 10.1109/TUFFC.2015.2495013

## II. Experimental Setup

A schematic of the QEPAS experimental setup employed in this work is shown in Fig. 1. A tunable continuous wave (CW), DFB quantum cascade laser (QCL, from Alpes Lasers #sbcw1422DN) was used as an excitation light source, operating at a wavelength of 6.23 μm, fixed in an ILX mount (model LDM-4872) equipped with a water cooling system and a short focal lens for beam collimation. The QCL operation temperature was set to $-7\,^{\circ}\mathrm{C}$ using a temperature controller (ILX Lightwave, LDT-5545B) and the laser was operated in CW mode by means of a current driver (ILX Lightwave, LDX-3232). At a current of 582.5 mA, we measured an output power of 10 mW. A $\mathrm{CaF_2}$ focusing lens $L_1$ with a focal length of 50 mm was used to couple the QCL output beam into a hollow core waveguide (HCW) to improve the QCL beam quality. The employed HCW is a circular cross-section glass capillary tube with a core diameter of 200 μm and a length of 15 cm and provides single-mode propagation with a Gaussian-like output beam profile [7]–[10]. $\mathrm{CaF_2}$ focusing optics $L_2$ is connected to the output of the fiber and provides a focusing distance of 38 mm [11], [12]. In the focal plane, an optical power of 1.2 mW was measured using a power meter, corresponding to HCW losses of $\sim 7\,\mathrm{dB}$. The QCL beam was coupled with the acoustic detection module (ADM) composed of a standard QTF and two acoustic organ pipe micro-resonator (MR) metal tubes (each 4-mm long and with inner diameter of 0.84 mm) [13].

The ADM was mounted inside a vacuum-thigh cell equipped with $\mathrm{CaF_2}$ windows. Standard air was pumped into the ADM using an oil-free vacuum diaphragm pump. Water vapor was

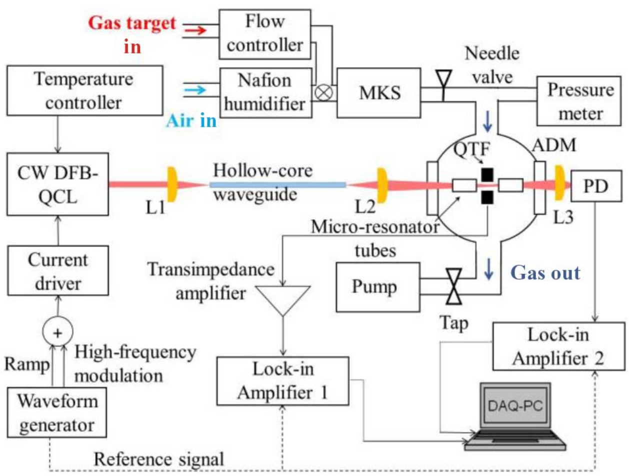


Fig. 1. Schematic of a CW DFB QCL-based QEPAS sensor. ADM, acoustic detection module; QTF, quartz tuning fork; PD, pyroelectric detector; $L_1, L_2, L_3, \mathrm{CaF}_2$ optical lenses.

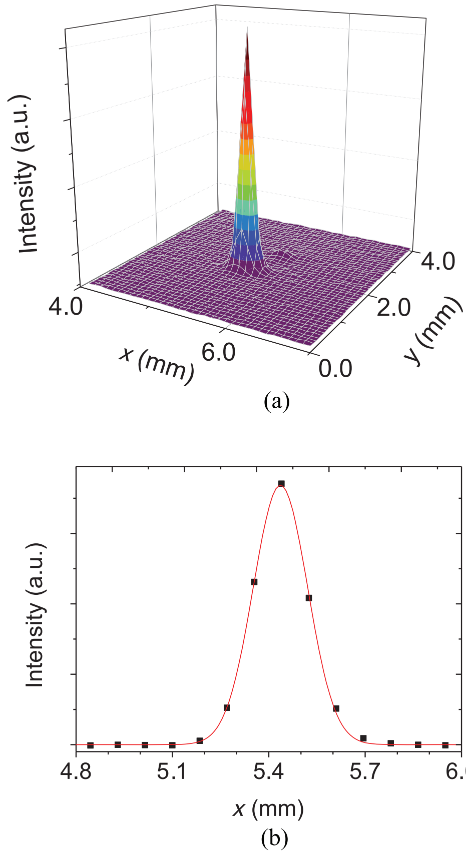


Fig. 2. (a) 3-D beam profile at the focal plane of the collimator and (b) corresponding 1-D profile with the related Gaussian fit (solid curve).

selected as the gas target for our investigation. A Nafion humidifier (PermaPure) and a hygrometer were connected to the gas line to set the water vapor concentration of the gas mixture at 3.1%. A needle valve and a tap were used to fix the gas pressure at an optimized value of 60 mbar, monitored by a digital pressure controller. At these operating conditions, we used a control electronic unit to determine the QTF parameters: the QTF resonant frequency $f_0 = 32\,763.38$ Hz, the quality factor $Q = 12\,600$, and the dynamic resistance $R = 91.5\,\mathrm{k}\Omega$. Wavelength modulation technique and $2f$-detection of the QEPAS signal were performed by applying a sinusoidal dither (with a peak-to-peak amplitude of 10 mA) to the QCL current at a frequency equal to $f_0/2$, using a waveform generator (Tektronix, AFG-3102). The piezoelectric current generated by the QTF was converted into a voltage signal by a transimpedance amplifier (with a feedback resistor of $10\,\mathrm{M}\Omega$); then, amplified by a gain of 30 and finally demodulated by a lock-in amplifier (lock-in Amplifier 1 in Fig. 1) at $f_0$. The output of the waveform generator acts as reference signal for the lock-in. Spectral profiles of the selected water vapor absorption line were obtained by slowly scanning the QCL wavelength by adding a voltage ramp to the QCL driver. We employed a triangular ramp voltage signal with an amplitude of $340\,\mathrm{mV_{pp}}$ and a frequency of 5 mHz. The QCL output coming from the ADM was focused by means of a $\mathrm{CaF}_2$ lens $L_3$ onto a pyroelectric detector (PD, VIGO PVI-3TE-6) and its response was demodulated at $f_0$ by a second lock-in amplifier (lock-in Amplifier 2 in Fig. 1), sharing the same reference signal with lock-in Amplifier 1. The two lock-in amplifiers were controlled by a National Instruments DAQ card connected to a personal computer for data acquisition. A DAQ acquisition time threefold the lock-in time constant was set for all measurements.

## III. Experimental Measurements

In the QEPAS technique, it is critical that the laser beam entering the MR tubes does not illuminate the tube walls and the QTF prongs to avoid photothermal effects and, consequently, a fringe-like nonzero background strongly limiting the QEPAS detection sensitivity [14], [15]. The three-dimensional (3-D) laser beam profile in the focusing plane of the collimator, acquired by a pyrocamera (Spiricon Pyrocam III) with pixel sizes of $0.085\,\mathrm{mm} \times 0.085\,\mathrm{mm}$, is shown in Fig. 2(a).

A one-dimensional (1-D) Gaussian-profile fit [Fig. 2(b)] yields an estimate of the average beam-waist diameter of $200\,\mu\mathrm{m}$, well below the QTF prongs spacing ($300\,\mu\mathrm{m}$) and the MR internal diameter. As a result, $>97\%$ of the laser beam was transmitted through the ADM leading to a negligible photothermal-induced background signal.

For a QEPAS-based sensor signal analysis, we selected a water vapor absorption line at $\lambda = 6.2371\,\mu\mathrm{m}$ with a line-strength $S = 4.481 \times 10^{-21}\,\mathrm{cm/mol}$, according to the HITRAN database [16]. Fig. 3 shows the QEPAS signal obtained by setting the lock-in time constant at 100 ms. The associated bandwidth is 1.6675 Hz with a 12-dB/oct filter slope. At a QCL current of 582.5 mA, the laser wavelength is resonant with the selected water absorption peak. For these conditions, we measured a QEPAS peak signal of 102.6 mV with a $1-\sigma$ noise of $95\,\mu\mathrm{V}$, corresponding to an SNR of 1080. Thus, starting from a 3.1% water concentration, the minimum detection limit (MDL) was determined to be $\cong 30$ part-per-million (ppm). A useful parameter to estimate the sensor performance is the noise equivalent absorption normalized to the laser power and the acquisition time (NNEA). We obtained an $\mathrm{NNEA} = 9.2 \times$

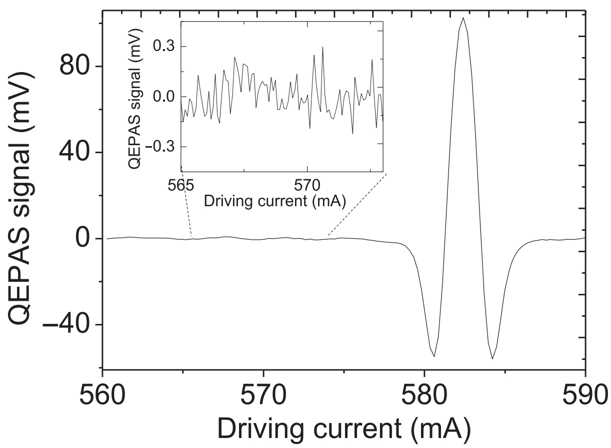


Fig. 3. Second-harmonic high-resolution QEPAS scans of standard air with a 3.1 % water vapor content. The QEPAS cell pressure was set to 60 mbar. The inset depicts the noise oscillations measured far from the QEPAS peak signal.

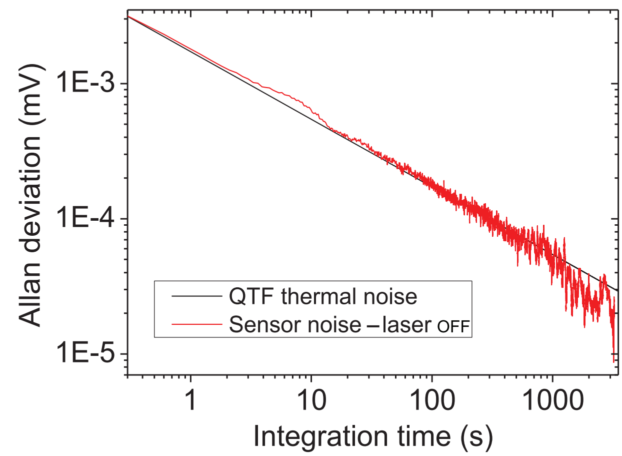


Fig. 4. Theoretical QTF thermal noise (black) and Allan deviation plot measured for the QEPAS sensor dark-noise signal (red), as a function of the integration time. The Allan deviation plot was rescaled by a factor 30 to take into account the transimpedance amplifier gain.

$10^{-9}$ W cm$^{-1}$ Hz$^{-1/2}$, which is a typical value for a QEPAS gas-sensing system [4].

## IV. QEPAS Sensor Allan Variance Analysis

To determine the long-term stability of a sensor system, an Allan variance analysis is mandatory. This analysis allows investigating drifts and establishing the sensor signal averaging limits. Given a set of $M$ time-series data acquired with an integration time $\tau$, its Allan variance $\sigma_y^2(\tau)$ is defined as

$$\sigma_y^2(\tau) = \frac{1}{M}\sum_{k=1}^{M}\frac{1}{2}(y_{k+1} - y_k)^2 \tag{1}$$

where $y_k$ is the $k$th-data averaged over an integration time $\tau$, $y_{k+1} - y_k$ is the difference between adjacent values of $y_k$, and $M$ is the total number of data, usually of the order of $10^3 - 10^4$. To estimate how $\sigma_y^2(\tau)$ changes with the integration time, we implemented a LabView-based code. Starting from the set of $M$ data acquired at an integration time $\tau_0$ and assuming that there is no dead time between adjacent measurements, the software averages the values for $y_1$ and $y_2$ and obtains a new $y_1$ value averaged over $2\tau_0$. Subsequently, this routine averages values for $y_3$ and $y_4$ and changes them as a new value $y_2$ averaged over $2\tau_0$ and finally applies (1) to determine $\sigma_y^2(2\tau_0)$. The software repeats this process for other integer multiples $m$ of $\tau_0$ and at the end of the processing, it generates values for $\sigma_y^2(m\tau_0)$ as a function of $(m\tau_0)$. Thus, to perform an Allan variance $\sigma_y^2$ analysis, all the data subsets have to be stacked together and treated as a single uninterrupted time sequence. Usually, the Allan deviation $\sigma_y$ is shown instead of the variance and expressed in terms of absorption coefficient or absorbing gas concentration; thus, determining the minimum detectable concentration as a function of the integration time.

In our experiments, each measurement lasted 4 h using a $2f$-wavelength modulation approach. However, prior to analyzing the stability of our sensor system, its fundamental noise limit must be determined. It is known that a QTF can be modeled as an RLC circuit [4]. The electrical response of the QTF is measured by means of a transimpedance amplifier with a gain resistor $R_g = 10$ MΩ. The root-mean-square of the QTF thermal (Johnson) noise is expressed as

$$\sigma_{\text{thermal}} = R_g\sqrt{\frac{2k_BT}{\pi R\tau}} \tag{2}$$

where $k_B$ is the Boltzmann constant, $T = 298$ K is the QTF temperature, and $\tau$ is the integration time. $R_g$ also introduces noise, which is several times lower than the thermal QTF noise and can be neglected for typical values of $R$ in the range 10–100 kΩ, as in our case. Thermal noise determines the MDL of the QEPAS sensor. If the QTF thermal noise is the dominant noise source, the Allan deviation closely follows a $1/\sqrt{t}$ dependence [see (2)], for the entire duration of the concentration measurements. To verify this assumption, a long-time acquisition of the QTF signal was performed in the absence of laser illumination (dark-noise). The acquired Allan deviation plot in mV is shown in Fig. 4, together with the expected thermal noise trend evaluated from (2). For comparison, the experimental data were rescaled by a factor 30, based on the transimpedance preamplifier gain.

The experimentally measured dark-noise dependence on the integration time matches the theoretically thermal one, thus confirming that for laser-OFF conditions only the Johnson noise influences the QEPAS sensor. The small hump between 2 and 10 s can be attributed to slow mechanical oscillations of the sensor system. The constant decrease in the Allan deviation over long integration times demonstrates that, in these conditions, the QEPAS sensor allows unlimited data averaging without base line or sensitivity drift. The next step was to investigate the sensor stability when the QCL is switched-ON. The QCL was electrically driven with a dc current plus a sinusoidal dither at $f_0/2$ and the QEPAS signal was acquired at $f_0$ by the lock-in Amplifier 1 (see Fig. 1). To determine the contribution of optical noise, for both *off-* and *on-resonance* conditions, we operated with the laser wavelength locked far from the water

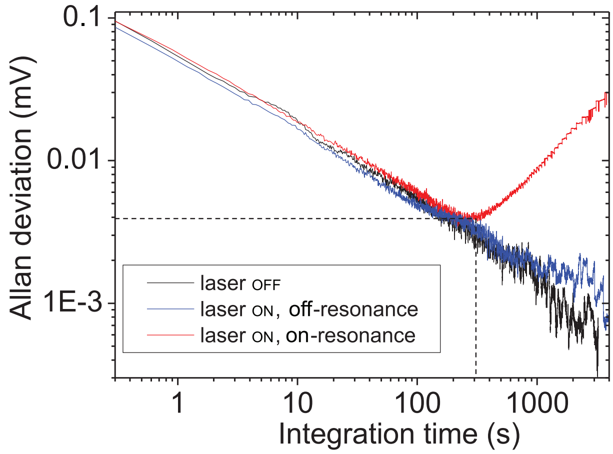


Fig. 5. Allan deviation plot in mV of the QEPAS sensor signal with laser-OFF (black curve), with the laser-ON and wavelength-locked far from the absorption line (*off-resonance*, blue curve), and with the laser-ON and locked-ON the water absorption wavelength peak (*on-resonance*, red curve), all as a function of integration time. The dashed lines mark the QEPAS-sensor optimum integration time of $\tau \sim 275$ s and the corresponding MDL of $\sim$1.2 ppm.

absorption line (at a dc current of 565 mA) or on its peak, respectively. The corresponding Allan deviations (in mV) of the QEPAS signal acquired under these two operating conditions, together with the previously measured dark noise, are shown in Fig. 5.

The Allan deviation measured for the *off-resonance* condition follows the Johnson noise trend and is almost identical to the QEPAS dark-noise, for an integration time of $\tau = 1000$ s. For longer integration times, a slight deviation is visible, implying that photothermal induced noise can play a role only at very long $\tau$, which are unrealistic for QEPAS operation. This result confirms the achievement of very good alignment and focusing conditions, due to the high quality of the HCW fiber-output laser beam. The Allan plot of the QTF signal for the *on-resonance* condition also follows the dark-noise trend, for an integration time of $\sim$275 s, where it reaches a minimum value of 3.7 $\mu$V. The conversion factor between the QEPAS signal in $\mu$V and ppm of water vapor concentration was $\sim$3.17 $\mu\mathrm{V/ppm}$; thus at $\tau \sim 275$ s, we reached a QEPAS sensor $\mathrm{MDL} \cong 1.2$ ppm. This minimum detection value corresponds to the turnover point of the Allan deviation plot; at longer $\tau$ values, the QEPAS sensitivity starts to deteriorate. The data of Fig. 5 suggest that this behavior may be related to laser intensity fluctuations when operating *on-resonance* condition. To verify this assumption, we performed an Allan deviation analysis of the laser power signal measured by the pyroelectric detector. The PD signal was acquired at $f_0$ by the lock-in Amplifier 2, for both laser-OFF (dark-noise) and laser-ON *on-resonance* operating conditions. The results are shown in Fig. 6.

For the QCL-OFF condition, the PD Allan deviation shows a Johnson noise $(1/\sqrt{t})$ trend for $\sim$1000 s integration times. For the QCL-ON condition, the noise level increased by at least one order of magnitude. A nearly flat-noise behavior is visible up to an integration time of 20 s, followed by a steady

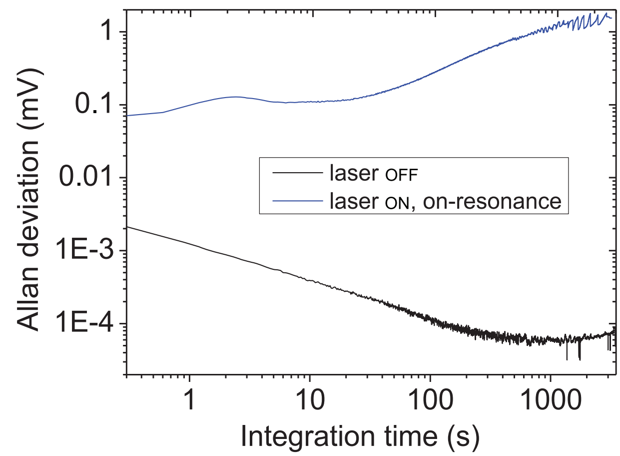


Fig. 6. Allan plot in mV of the PD noise when the QCL is OFF (black), and when the QCL is ON and the sensor is locked on the $H_2O$ absorption line peak (*on-resonance*, blue).

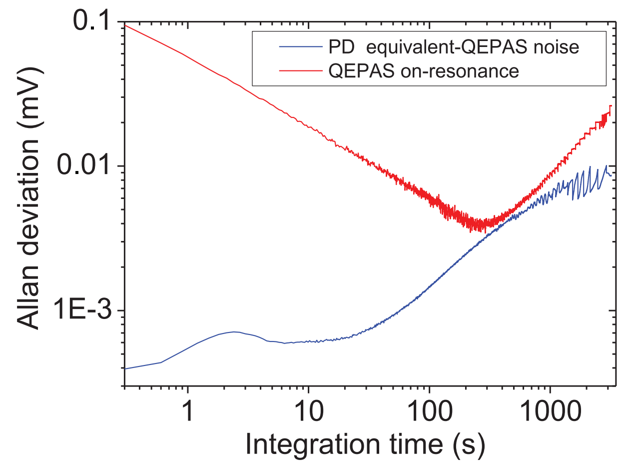


Fig. 7. Allan deviation of the PD equivalent-QEPAS noise (blue curve) and of the QEPAS sensor *on-resonance* (red curve) as a function of the integration time.

noise level increase with $\tau$. The small hump between 2 and 10 s can be attributed to slow mechanical oscillations of the system.

The Allan deviation analysis demonstrates that QCL-related power fluctuations dominate the PD noise signal, especially at long integration times.

To investigate how laser fluctuations affect the QEPAS noise, we converted the PD noise into laser power fluctuations and subsequently extracted the related equivalent-QEPAS noise contribution. The conversion factor between the PD signal and the laser optical power was 70 $\mu\mathrm{W/V}$. To convert laser power into a QEPAS signal, we used a conversion factor of 85.5 mV/mW (for an optical power of 1.2 mW, we measured a QEPAS peak signal of 102.6 mV, see Fig. 3). In Fig. 7, we compared the PD equivalent-QEPAS noise Allan deviation with the measured QEPAS sensor *on-resonance*.

The results show that, for $\tau < 275$ s, the contribution to the QEPAS noise due to the laser power fluctuations is negligible and QTF thermal noise dominates. However, for longer integration times, laser power instabilities contribute with the photothermal induced noise to the increase in the QEPAS noise level, compromising the system stability and hence decreasing the MDL of the reported sensor system.

## V. Conclusion

In summary, we demonstrated the merits of employing the Allan variance analysis to investigate the long-time stability of a QEPAS-based sensor system and particularly in providing information about the optimum averaging time and predicting the achievable MDLs.

It was shown that the sensor noise is dominated by the QTF thermal noise up to $\tau \cong 275\,\text{s}$. For longer integration times, laser power instabilities become the main noise source and a steady noise level increase is observed. Therefore, one has to reduce the laser power fluctuations to improve the sensor sensitivity. This will require the implementation of more stable laser current driver and temperature controller technologies.

## References

[1] J. Hodgkinson and R. P. Tatam, "Optical gas sensing: A review," *Meas. Sci. Technol.*, vol. 24, pp. 012004:1–012004:59, 2013.

[2] A. Elia, P. M. Lugarà, C. di Franco, and V. Spagnolo, "Photoacoustic techniques for trace gas sensing based on semiconductor laser sources," *Sensors*, vol. 9, pp. 9616–9628, 2009.

[3] A. A. Kosterev, F. K. Tittel, D. Serebryakov, A. Malinovsky, and A. Morozov, "Applications of quartz tuning fork in spectroscopic gas sensing," *Rev. Sci. Instrum.*, vol. 76, pp. 043105:1–043105:9, 2005.

[4] P. Patimisco, G. Scamarcio, F. K. Tittel, and V. Spagnolo, "Quartz-enhanced photoacoustic spectroscopy: A Review," *Sensors*, vol. 14, pp. 6165–6206, 2014.

[5] D. W. Allan, "Statistics of atomic frequency standards," *Proc. IEEE*, vol. 54, no. 2, pp. 221–230, Feb. 1966.

[6] P. Werle, R. Miicke, and F. Slemr, "The limits of signal averaging in atmospheric trace-gas monitoring by tunable diode-laser absorption spectroscopy (TDLAS)," *Appl. Phys. B*, vol. 57, pp. 131–139, 1993.

[7] P. Patimisco *et al.*, "Coupling external cavity mid-IR quantum cascade lasers with low loss hollow metallic/dielectric waveguides," *Appl. Phys. B*, vol. 108, pp. 255–260, 2012.

[8] A. Sampaolo, P. Patimisco, J. M. Kriesel, F. K. Tittel, G. Scamarcio, and V. Spagnolo, "Single mode operation with mid-IR hollow fibers in the range 5.1–10.5 µm," *Opt. Exp.*, vol. 23, pp. 195–204, 2015.

[9] M. Siciliani de Cumis *et al.*, "Widely-tunable mid-infrared fiber-coupled quartz-enhanced photoacoustic sensor for environmental monitoring," *Opt. Exp.*, vol. 22, pp. 28222–28231, 2014.

[10] P. Patimisco *et al.*, "Low-loss hollow waveguide fibers for mid-infrared quantum cascade laser sensing applications," *Sensors*, vol. 13, pp. 1329–1340, 2013.

[11] V. Spagnolo, P. Patimisco, S. Borri, G. Scamarcio, B. E. Bernacki, and J. Kriesel, "Part-per-trillion level SF6 detection using a quartz enhanced photoacoustic spectroscopy-based sensor with single-mode fiber-coupled quantum cascade laser excitation," *Opt. Lett.*, vol. 37, pp. 4461–4463, 2012.

[12] V. Spagnolo, P. Patimisco, S. Borri, G. Scamarcio, B. E. Bernacki, and J. Kriesel, "Mid-infrared fiber-coupled QCL-QEPAS sensor," *Appl. Phys. B*, vol. 112, pp. 25–33, 2013.

[13] L. Dong, A. A. Kosterev, D. Thomazy, and F. K. Tittel, "QEPAS spectrophones: Design, optimization, and performance," *Appl. Phys. B*, vol. 100, pp. 627–635, 2010.

[14] V. Spagnolo, A. A. Kosterev, L. Dong, R. Lewicki, and F. K. Tittel, "NO trace gas sensor based on quartz-enhanced photoacoustic spectroscopy and external cavity quantum cascade laser," *Appl. Phys. B*, vol. 100, pp. 125–130, 2010.

[15] L. Dong, V. Spagnolo, R. Lewicki, and F. K. Tittel, "Ppb-level detection of nitric oxide using an external cavity quantum cascade laser based QEPAS sensor," *Opt. Exp.*, vol. 19, pp. 24037–24045, 2011.

[16] HITRAN database [Online]. Available: www.hitran.org (accessed Jun. 5, 2015).

**Marilena Giglio** received the M.S. degree (*cum laude*) in applied physics from the University of Bari, Bari, Italy, in 2014, where she is currently pursuing the Master's degree in mechatronics since 2014.

She is currently a Research Assistant with the Department of Physics, University of Bari. Her research interests include optical coherence tomography (OCT) as an imaging technique for thin tissues, the analysis of the parameters of speckle distribution in OCT B-scans, and development of gas sensors based on quartz-enhanced photoacoustic spectroscopy.

**Pietro Patimisco** received the Master's (*cum laude*) and Ph.D. degrees from the University of Bari, Bari, Italy, in 2009 and 2013, respectively, both in physics.

Since 2013, he has been a Postdoctoral Research Assistant with the University of Bari. He was a Visiting Scientist at the Laser Science Group, Rice University, Houston, TX, USA, from 2013 to 2014. His research interests include micro-probe optical characterization of semiconductor optoelectronic devices and optoacoustic gas sensors, the study and applications of trace-gas sensors, such as quartz-enhanced photoacoustic spectroscopy and cavity-enhanced absorption spectroscopy in the mid-infrared and terahertz spectral region, leading to several publications, including a cover paper in the July 2013 issue of *Applied Physics Letters*.

**Angelo Sampaolo** received the Master's degree in physics from the University of Bari, Bari, Italy, in 2013, where he is currently pursuing the Ph.D. degree in physics.

Since September 2014, he has been a Research Assistant with the Laser Science Group, Rice University, Houston, TX, USA. His research interests include the study of the thermal properties of heterostructured devices via Raman spectroscopy, development of innovative techniques in trace gas sensing, based on quartz-enhanced photoacoustic spectroscopy and covering the full spectral range from near-IR to THz. His achieved results have been acknowledged by a cover paper in the July 2013 issue of *Applied Physics Letters*.

**Gaetano Scamarcio** received the Ph.D. degree in physics from the University of Bari, Bari, Italy, in 1989.

Since 2002, he has been a Full Professor of Experimental Physics, University of Bari. From 1989 to 1990, he was a Research Fellow with Max-Planck-Institute für Festkörper-forschung, Stuttgart, Germany, and a Visiting Scientist at Walter-Schottky-Institute, Garching, Germany, in 1992. From 1994 to 1996 and from 2000 to 2001, he was a Visiting Scientist at Bell Laboratories, Lucent Technologies (formerly AT&T), Murray Hill, NJ, USA. In 2006, he was an Invited Professor at the University of Paris 7, Paris, France. His research interests include the development and applications of quantum cascade lasers, optical, vibrational and transport properties of semiconductor structures at the nanoscale, spectroscopic techniques for real-time monitoring of optoelectronic devices, optoelectronic sensors for mechatronics.

Dr. Scamarcio received the Italian Physical Society Award in 1989, the Firestone Prize for Young Laureates in 1985, and an NATO-CNR Advanced Fellowship in 1995.

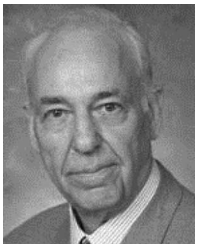

**Frank K. Tittel** received the Master's and Doctorate degrees from the University of Oxford, Oxford, U.K., in 1955 and 1959, respectively, both in physics.

From 1959 to 1967, he was a Research Physicist with the General Electric Research and Development Center, Schenectady, NY, USA. Since 1967, he has been the Faculty of the Department of Electrical and Computer Engineering and Biomedical Engineering, Rice University, Houston, TX, USA, where he currently an Endowed Chaired Professor. His research interests include various aspects of quantum electronics, in particular laser spectroscopy and laser applications in environmental monitoring, atmospheric chemistry, industrial process control, and medical diagnostics.

Dr. Tittel is a Fellow of the Optical Society of America, the American Physical Society, and SPIE.

**Vincenzo Spagnolo** received the Ph.D. degree in physics from the University of Bari, Bari, Italy, in 1994.

From 1997 to 1999, he worked as Researcher with the National Institute of the Physics of Matter (INFM). From 1999 to 2003, he was a Postdoctoral Research Associate with the Department of Physics, University of Bari. Since January 2004, he has been an Assistant Professor with the Department of Physics, Polytechnic of Bari, Bari, Italy. His research activity is documented by more than 130 publications and 2 filed patents. He has given more than 30 invited presentations at international conferences and workshops. His research interests include quantum cascade lasers, spectroscopic techniques for real-time device monitoring, optoacoustic gas sensors.

Dr. Spagnolo is a Senior Member of the SPIE.